(C)

2016   2018

Development and application of intra-resonator coherent beam combination
technique using an axicon as a retro-reflective mirror

Chosrowjan, Haik

3,800,000

AL   CCR
CW
CW

The possibility of generating high-power and high-beam quality radiation directly from the resonator
 based on total reflection active mirror laser medium was evaluated.
Lasing characteristics of axicon lens with 90 degrees apex angle and corner-cube retro-reflector
resonators have been studied.

            High power, high brightness CW lasers with good beam quality are required
for applications in material processing, environment monitoring, etc. Most high power solid-state
laser developments occur based on the concept of master oscillator power amplifier. We explored the
possibility of generating high power CW beams directly from the laser oscillator by using Axicon
lens (AL) and corner-cube (CCR) retroreflectors as total reflection elements in the resonator.
Polarization and lasing characteristics of AL and CCR resonators have been studied theoretically and
 experimentally. Several characteristics of resonators with retro-reflecting elements have been
recognized. Laser threshold and slope efficiencies were estimated at cryogenic and ambient
temperatures. It was revealed that the coherence of the AL resonator output cannot be studied for
the TRAM configuration because the beam polarization is elliptical and could not be controlled due
to phase jumps caused by total internal reflection.

Axicon lens Corner-cube reflector Axicon resonator CCR resonator Passive CBC

様　式　Ｃ－１９、Ｆ－１９－１、Ｚ－１９、ＣＫ－１９（共通）

1．研究開始当初の背景

(1) High power, high brightness lasers with good beam quality are increasingly required for many applications in material processing, environment monitoring, etc. Efforts are made to develop multi-kilowatts (kW) average power, high beam quality coherent radiation sources. The easiest way to get the desired multi kW output power would be generating it directly from the laser resonator. However, scaling beam power directly from laser resonators has proven to be a difficult task due to thermal problems and mechanical stress in the active medium. Hence, most high-power solid-state laser developments occur based on a concept of master oscillator power amplifier (MOPA). In this concept, a seed beam is amplified in a multi-pass amplifier-chain system. Irrespective of the active medium, it is easy to show that highest possible amplification efficiency for a given system can be reached when the pump- and seed beams both have flattop phase and intensity profiles. Unfortunately, available lasers which can be used as such seed beams, have moderate power and Gaussian profile, which reduces the amplification efficiency due to insufficient mode matching of the pump- and seed beams. In this research project we explored the possibility of generating high-power CW beam with flattop-like profile directly from the laser resonator. Such laser, if successful, could be used as an effective seed laser for multi-stage amplifiers in multi-kilowatts operating regime.

２．研究の目的

(1) The purpose of this research was obtaining high-power coherent radiation with flattop-like beam profile directly from a laser resonator based on cryogenic Yb^{3+}:YAG TRAM (total reflection active mirror) configuration. It is achieved by employing a special retro-reflective element (an axicon lens (AL) with 90 degrees apex angle or a corner-cube retroreflector (CCR)) used as a total reflection mirror in the resonator.

３．研究の方法

(1) In this project polarization properties and lasing characteristics of AL and CCR resonators have been studied theoretically and experimentally. We have built a laser resonator based on cryogenic Yb:YAG TRAM with exchangeable high reflection elements: a flat mirror, a CCR and an AL. We have pumped the system using a laser diode (LD) with flattop intensity profile and investigated the output power efficiency vs. the pump power and near- and far-field intensity profiles. Efforts were made to measure the beam parameter product (M2) and phase wave-front distortions, too. Model calculations of resonator eigenmodes have been done to support the findings. The potential of the axicon as a high reflection mirror in the resonator has been elucidated.

４．研究成果

(1) Corner-cube retroreflectors (CCR) and axicon lenses (AL) are optical components with interesting reflective and polarization characteristics. One of their properties is that the collimated radiation incident on both elements (arbitrary direction for CCR and normal incident for the axicon with 90 degrees apex angle) is reflected in the direction that is counter-parallel to the incident beam. Another common property of both elements is that the reflected beam has coherent properties, which could be used for passive intra-resonator coherent beam combining (CBC). Recently we have suggested that axicons with 90 degrees apex angle can be also used for such purpose. Moreover, using axicons as total reflection mirrors, it seems to be possible generating beams with radial- or tangential polarizations.

(2) Detailed knowledge of intensity distributions of p- and s- polarization components in retro-reflected beam is essential for designing and building resonators with retro-reflective components. Moreover, polarization properties of retro-reflected beams are also essential for modeling laser mode formation inside the resonator. So, we have studied experimentally the basic polarization and reflection properties of corner-cube and axicon retroreflectors. Experimental results of near- and far-field intensity distributions for depolarized, p- and s- polarized outputs of these elements are presented and analyzed. We have performed also case-calculations for several polarization states based on Fresnel equations and compared them with the experiments.

(3) CCRs and ALs are often fabricated using fused silica or various glass materials. For achieving retro-reflection of an optical beam, one can coat the reflective surfaces with different metallic or dielectric substrates or simply use them with well-polished but uncoated surfaces. In the later case the total internal reflection (TIR) phenomenon, characterized by critical incidence angle $\theta_c = arcsin(n_2/n_1)$, where $n_2 < n_1$, is used for the incidence beam retro-reflection. For high-power laser beam applications, retroreflectors with coated surfaces are not appropriate because of anticipated thermal degradation and damage of the coated surfaces. Hence, we studied polarization and reflection properties of a CCR (N-BK7 glass, n = 1.5071 at 1030 nm, θ_c = 41.57 degrees) and an AL with 90 degrees apex angle (fused silica, n = 1.45 at 1030 nm, θ_c = 43.6 degrees) based on the TIR phenomenon. Briefly, reflection of p- and s- polarized light at the interface between two homogeneous and isotropic media is governed by well-known Fresnel equations. When both media are transparent, the phase shifts that accompany partial *external* or *internal* reflections assume the values of π or 0. However, under TIR conditions at angles of

incidence θ above the critical angle θ_c, the phase shifts are nontrivial and given by the following equations:

$$tan(\delta_p/2) = N\sqrt{N^2sin^2\theta - 1}/cos\theta \qquad (1) \qquad ; \qquad tan(\delta_s/2) = \sqrt{N^2sin^2\theta - 1}/(Ncos\theta) \qquad (2)$$

Here δ_p and δ_s are the phase shifts of p- and s- polarized waves, respectively, θ is the incidence angle and $N = n_1 / n_2 > 1$, is the high-to-low ratio of the refractive indices of the incidence and refraction (evanescent) media, respectively.

(4) We have performed several case-calculations for an axicon lens with 90 degrees apex angle, but present results of only two of them (p- and radial polarized cases) in this report due to the space limitations. Calculated intensity distribution profiles of p- and s- polarized components reflected from the AL for p- polarized incident beam with Gaussian intensity distribution profile are presented in the Fig. 1 (a), while for radial polarized incidence beam with Gaussian intensity distribution profile the results are presented in the Fig. 2 (b).

Fig. 1 (a) p- polarized incidence beam intensity distribution profile (left) and intensity distribution profiles of its p- (middle) and s-polarization (left) components reflected from the AL; **(b)** Radial polarized incidence beam intensity distribution profile (left) and intensity distribution profiles of its p- (middle) and s-polarized (left) components reflected from the AL. Red arrows indicate the polarization directions in each case.
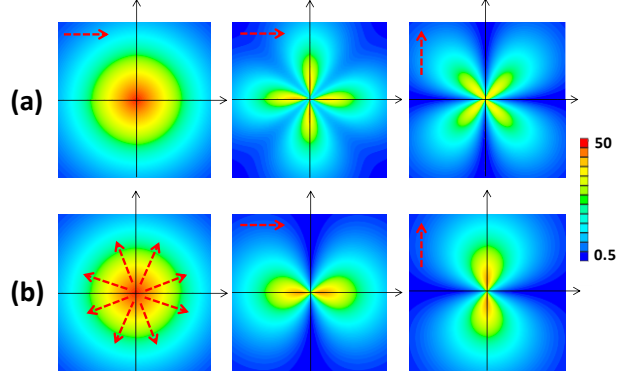
In Fig. 2 (a) and (b) calculated p- and s- components intensity distribution profiles and $\Delta\delta_{s-p}$ phase differences versus the azimuth angle α in the $0 \le \alpha \le \pi/2$ interval for p- and radial polarized incidence beams, respectively, are presented. Note that due to the axial symmetry of the AL, the rays entering, for instance, the upper right quarter exit the AL from the lower left quarter, and so on. From the phase relations it is clearly seen that in AL resonator a linearly polarized beam after retro-reflection from the AL will be depolarized (becomes locally elliptically polarized) and cannot be invariant (keep its polarization) after a round trip. In other words, there will be always both p- and s-polarized beam components in the resonator and no polarization selection is possible. This conclusion is also valid for ALs with polarization maintaining ($\delta_s = 0$) metal coated reflection surfaces.


Fig. 2 Amplitudes of the AL reflected beam's p- and s- intensity components (black) and phase difference $\Delta\delta_{s-p}$ (red) dependences on the azimuth angle α in the $0 \le \alpha \le \pi/2$ interval: **(a)** The incidence beam is p- polarized plane wave with Gaussian intensity distribution profile; **(b)** The incidence beam is a radial polarized beam with Gaussian intensity distribution profile. For both cases the incidence- and emerging ray polarizations at (x, y) and (-x, -y) points, respectively, are schematically shown on the right panels of the corresponding figures.
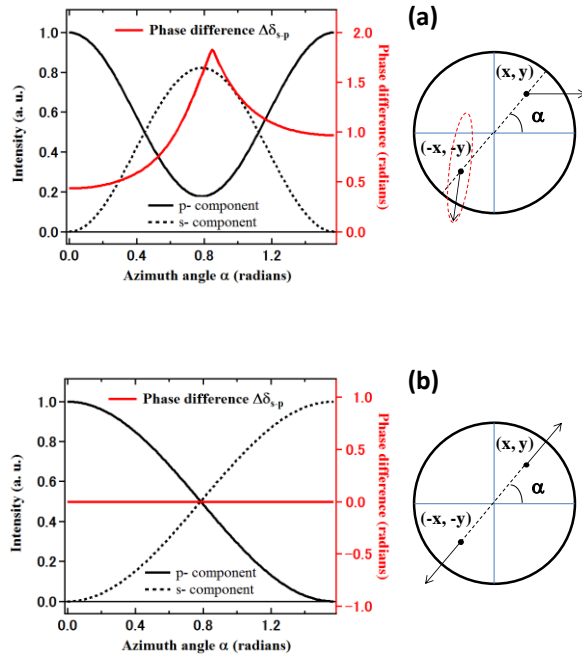
On the other hand, in AL resonator a radial polarized beam after retro-reflection from the AL keeps its polarization invariant (phase difference between p- and s- components is zero) after a round trip. In other words, the eigenmode of the resonator with AL has radial polarized component. This conclusion is also valid for ALs with polarization maintaining ($\delta_s = 0$) metal coated reflection surfaces.

(5) An experimental setup to test the reflection properties of the AL and CCR was built and tested. On Fig. 3 measurement results for AL are presented. Comparison of the Fig. 3 and Fig. 1 (a) reveals that the calculations match quite well with the experiments, A singularity observed in the center of the images is due to the diffraction on the apex tip of the axicon lens not taken into consideration in the calculations.

Fig. 3 Intensity distribution profiles of p- polarized incidence beam reflected from the AL: depolarized- (left), p-polarized (middle) and s- polarized components (right), respectively;
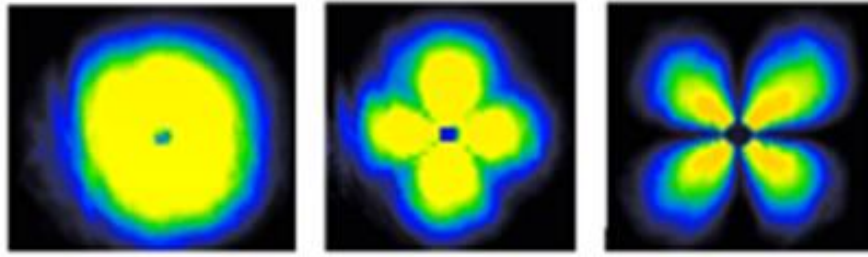
(6) We have constructed AL and CCR based resonators and compared the results with conventional Fabry-Perrot (FP) resonator. Lasing threshold, slope efficiency, near- and far-field intensity distribution profiles have been monitored. Passive CBC effect inside the CCR resonator was demonstrated based on experimental results and mode calculations. The experimental resonator setup used in this study is schematically illustrated in Fig. 4. Cryogenically (LN₂) cooled Yb:YAG total reflection active mirror (TRAM) with 9.8 at % doped ytterbium and d = 0.2 mm thickness was used as an active medium. The total length of the resonator was set to be 460 mm while the LD excitation (P_{max} ~ 200 W) spot was kept at ~ 1.8 mm in diameter. On the other hand, 9.8 at% doped Yb:YAG TRAM with d = 0.6 mm thickness was used as an active medium in lasing experiments at ambient temperature. The LD excitation (P_{max} ~ 600 W) spot was kept at ~ 5 mm in diameter.
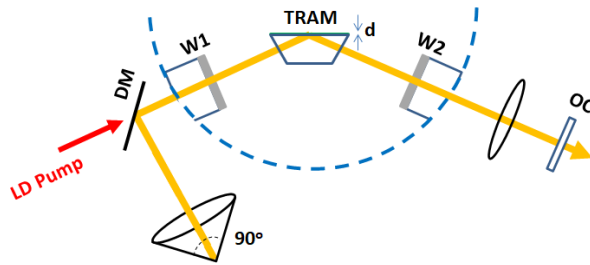

Fig. 4 Experimental setup for comparative investigations of lasing characteristics for AL, CCR and FP resonators: DM – dichroic mirror, W1, W2 – cryostat windows, OC – output coupler, TRAM – total reflection active mirror, d – Yb doped layer thickness. The cryostat perimeter is marked with the dotted line.

In Fig. 5 the laser output power versus the absorbed pump power for AL, CCR and FP resonators at cryogenic temperatures are presented. In these experiments the same 80 % reflective output coupler (OC) was used. The laser threshold and the slope efficiencies were measured to be about 0.7 kW/cm² and 0.5 for the FP resonator, 1.15 kW/cm² and 0.4 for AL, and 1.5 kW/cm² and 0.33 for the CCR resonators, respectively. The maximum output power achieved from the AL and CCR resonators was ~ 24 W and 17.5 W, respectively. The obtained slope efficiency for FP resonator matches well with our previous result of 0.525 using 84.6 % reflective OC. An AL or CCR laser based on TRAM was constructed for the first time, so no effective comparisons can be made at this stage. Marked increase of the laser threshold and decrease of the slope efficiencies for AL and CCR resonators are explained by the small beam diameter on those elements, incurring fractionally large losses due to scattering on the tip of the AL and three corners of the CCR, respectively.


Fig. 5 Output- vs. absorbed pump power dependences for lasers with conventional- (mirror), AL and CCR high-reflective elements, respectively.
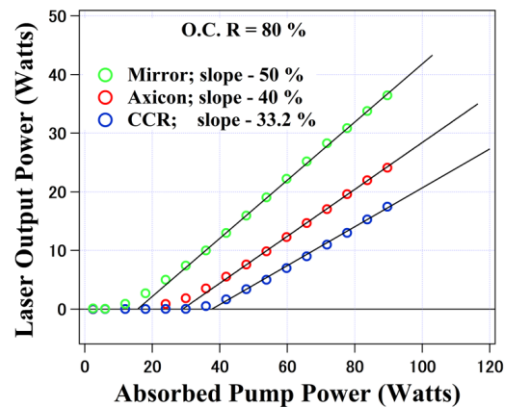
In Fig. 6, NF and FF output intensity distributions of FP, AL and CCR resonators for two absorbed pump power cases are shown. It is seen that thermal effects up to 90 W absorbed pump power hardly affect the main features of the beam profiles.

**Fig. 6** NF (top) and FF (bottom) intensity distribution patterns of a FP (right), AL (middle) and CCR (left) laser beams for 55 W and 90 W absorbed pump power cases, respectively.

Resonator type	Mirror		Axicon		CCR	
Absorbed power	55 W	90 W	55 W	90 W	55 W	90 W
NF						
FF						

Based on resonator configuration one can also deduce that the FP resonator
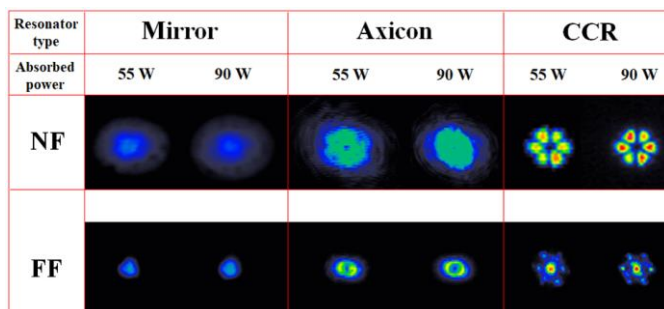
operates at multi-mode regime. On the other hand, although the NF intensity profiles for the CCR resonator look like the higher order TEM_{03} Laguerre-Gaussian mode (LG03), the FF patterns show a strong symmetrical central peak surrounded by six weaker peaks. There have been different opinions for the reason why a CCR can contribute to improve the laser FF power focalization. Some considered the CCR resonator output to be a LG03 mode based solely on the NF profile of the output beam, while some thought that the FF intensity distribution possesses quasi-phase conjugate characteristics. To clarify the origin of the CCR resonator output, we have performed model calculations of mode characteristics of CCR resonators based on Jones matrix formalism and Fresnel-Kirchhoff diffraction integral equation, and present obtained results in Fig. 7 together with the experimental results. Calculated NF and FF profiles of higher order TEM_{03} Laguerre-Gaussian mode (LG03) are also presented for better comparison.

Fig. 7 (a column) Calculated NF and FF profiles of the TEM_{03} (LG03) mode; **(b** column) calculated, and **(c** column) measured NF and FF profiles of CCR resonator output.
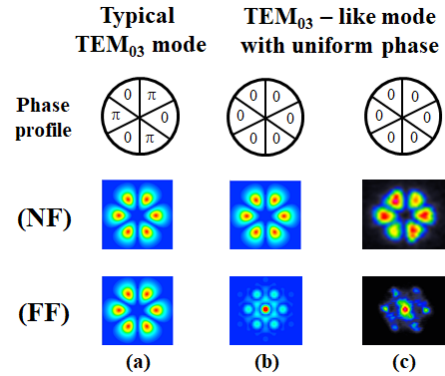
When a CCR is viewed along a symmetric optical axis, the NF distribution of the output beam is seen to be divided into six fan-shaped segments by three reflected surfaces and edges of the CCR. The NF profiles of the **(a)** and **(b)** columns in Fig. 7 are identical. However, the calculated and measured FF patterns of the CCR resonator unambiguously demonstrate that the CCR resonator output is not a LG03 mode. The six separated beam parts are coherent (in-phase), indicating the coherent nature of the CCR reflected beams and hence, possibility of passive intra-resonator coherent beam combination (CBC), when a CCR is used as a high reflection element. The CCR based passive CBC in bulk solid-state lasers is especially promising for obtaining high energy pulsed beams, because in fiber laser based active CBC it is difficult to achieve high energy pulsed outputs.

One of potential merits using AL or CCR instead of a mirror in the resonator was based on the earlier observations that at higher excitation powers the FP laser output undergoes a thermal roll-over, so application of AL or CCR could possibly improve that detrimental thermal effect. However, in the available TRAM sample (d = 0.2 mm) the pump power ($P_{max} \sim 200$ W) absorption ratio was only 0.45 and the thermal roll-over effect has not appeared at cryogenic temperatures. To explore potential benefits of the AL and CCR resonators, we have performed also lasing experiments at ambient temperature. The resonator configuration was similar to the case when cryogenic cooling was applied, however, in experiments at ambient temperatures the cryostat was removed, and the TRAM was installed on a water jet impingement cooling system. In all experiments at ambient temperature the same 90 % reflective OC was used. The laser threshold and the slope efficiency for the FP resonator, both could be only roughly estimated to be larger than 720 W/cm^2 and 0.3, respectively. This uncertainty is due to the nonlinear dependence of the output- vs. absorbed pump powers caused by the reabsorption effect of Yb^{3+} ion at around 1030 nm lasing wavelength. On the other hand, for the AL resonator, even rough estimation of the lasing slope and threshold could not be made due to the inefficient and weak laser output. The reason for marked increase of the laser threshold and anticipated decrease of the slope efficiency for AL vs. FP resonators at ambient temperatures can be only partly explained by the fractionally large losses due to scattering on the tip of the AL. Additional experiments are required for understanding the true nature of the lasing efficiency drop in AL resonator case at ambient temperature. No lasing could be observed for the CCR resonator at ambient temperature. Lasing performance comparison between cryogenic and ambient temperature cases reveals that the lasing efficiency, as expected, is lower for the later due to regressive material properties of Yb:YAG and reabsorption increase from low- to higher temperatures.

Concerning the beam quality, we have tried measuring the beam quality factor M^2 for FP and AL resonator outputs (4-σ ISO-standard method, measured by BC106N-VIS/M (Thorlabs) instrument). For FP resonator at ~ 8 W output, the M^2 factor for X- and Y- directions were 11.84 and 8.32 (M^2 mean ~ 9.92), respectively.
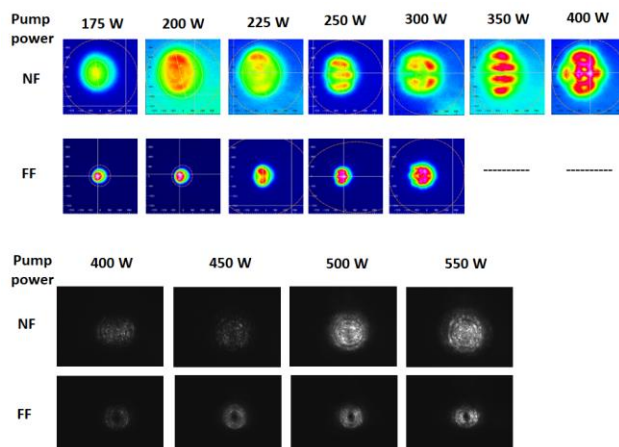

Fig. 8 (top) NF and FF profiles of laser beam from FP resonator at different pump powers; **(bottom)** NF and FF profiles of laser beam from AL resonator at different pump powers.

As the laser pump/output power increased, the multi-mode operation of the laser dominated and no reasonable measurements of M^2 factor could be performed.

In case of the AL resonator, unfortunately, M^2 factor measurements were unsuccessful. This could be caused by the donut-like beam profile of the AL resonator output. To compare qualitatively the beam qualities of FP and AL resonator outputs, an indirect method was adopted. Namely, beam profile changes in near- and far-fields at increasing pump powers (increasing thermal load in TRAM active medium) were monitored and compared. Based on resonator configuration (no mode selection elements involved) one can deduce that the FP resonator will operate at multi-mode regime as the pump power increases. Indeed, at increasing pump powers (Fig. 8, top raw), the NF and FF profiles continuously change, indicating that the resonator enters a multi-mode regime (higher order resonator modes are not suppressed). On the other hand, for AL resonator even at higher pump powers the NF and FF profiles do not change, indicating that intra-resonator mode selection occurs, and high order resonator modes are suppressed (Fig. 8, bottom raw).

Unfortunately, the coherence properties of the AL resonator output cannot be studied for the particular case of TRAM active medium configuration. This is because the output beam polarization for TRAM configuration cannot be controlled due to the phase jumps caused by total internal reflection.

５．主な発表論文等

〔雑誌論文〕（計５件）
① H. Chosrowjan and S. Taniguchi, Polarization and Reflection Characteristics of an Axicon Lens, Annual Progress Report of the Institute for laser Technology (ILT2017), 査読無, 29, 2017, 14 – 19
② H. Chosrowjan and S. Taniguchi, Laser Characteristics of Corner-Cube Retroreflector Resonators, Annual Progress Report of the Institute for laser Technology (ILT2018), 査読無, 30, 2018, 17 – 20
③ H. Chosrowjan and S. Taniguchi, Laser Characteristics of Axicon Retroreflector resonator, Annual Progress Report of the Institute for laser Technology (ILT2019), 査読無, 31, 2019, in press
④ H. Chosrowjan, S. Taniguchi, H. Yoshida and N. Miyanaga, Polarization and Laser Properties of Resonators with Corner-Cube and Axicon Retroreflectors, Proceedings of the 7th Advanced lasers and Photon Sources (ALPS'18), 査読有, 7, 2018, 1 – 2
⑤ G. Khosrovian, S. Taniguchi, H. Yoshida and N. Miyanaga, Lasing Characteristics of Resonators with Retroreflective Elements, IEEE Xplore Digital Library, 査読有, 2018, 73 – 74
DOI:10.1109/LO.2018.8435216

〔学会発表〕（計７件）
① H. Chosrowjan, S. Taniguchi, and T. Kitamura, Polarization properties of corner-cube and axicon retroreflectors, 第 64 回応用物理学会春季学術講演会、14p-P6-10, 2017
② H. Chosrowjan and S. Taniguchi, Laser characteristics of corner-cube retroreflector resonator, 第 78 回応用物理学会秋季学術講演会、6p-PA1-5, 2017
③ H. Chosrowjan and S. Taniguchi, Laser characteristics of axicon retroreflector resonator, 第 65 回応用物理学会春季学術講演会、18p-P1-4, 2018
④ H. Chosrowjan, S. Taniguchi and N. Miyanaga, Laser characteristics of corner-cube and axicon retroreflector resonators, 第 79 回応用物理学会秋季学術講演会、20a-PB2-3, 2018
⑤ H. Chosrowjan, S. Taniguchi, and N. Miyanaga, Laser characteristics of corner-cube and axicon retroreflector resonators at cryogenic and ambient temperatures, 第 66 回応用物理学会春季学術講演会、11a-PA4-4, 2019
⑥ H. Chosrowjan, S. Taniguchi, H. Yoshida and N. Miyanaga, Polarization and Laser Properties of Resonators with Corner-Cube and Axicon Retroreflectors, OPIC2018, ALPS'18, The 7th Advanced Lasers and Photon Sources International Conference, ALPSp-16, Yokohama, 2018
⑦ G. Khosrovian, S. Taniguchi, H. Yoshida and N. Miyanaga, Lasing Characteristics of Resonators with Retro-Reflective Elements, 18th International Conference Laser Optics 2018 (ICLO2018), WeR1-p47, St. Petersburg, Russia, 2018

〔その他〕
① http://www.ilt.or.jp/pdf/lasercross-paper/no353.pdf
② http://www.ilt.or.jp/pdf/lasercross-paper/no365.pdf
③ http://www.ilt.or.jp/pdf/lasercross-paper/no372.pdf

６．研究組織

(1)研究協力者
研究協力者氏名：谷口　誠治
ローマ字氏名：(TANIGUCI seiji)